Scaling the Ion Trap Quantum Processor

C. Monroe and J. Kim

Science **339**, 1164 (2013);
DOI: 10.1126/science.1231298

REVIEW

Scaling the Ion Trap Quantum Processor

C. Monroe[1]* and J. Kim[2,3]

Trapped atomic ions are standards for quantum information processing, serving as quantum memories, hosts of quantum gates in quantum computers and simulators, and nodes of quantum communication networks. Quantum bits based on trapped ions enjoy a rare combination of attributes: They have exquisite coherence properties, they can be prepared and measured with nearly 100% efficiency, and they are readily entangled with each other through the Coulomb interaction or remote photonic interconnects. The outstanding challenge is the scaling of trapped ions to hundreds or thousands of qubits and beyond, at which scale quantum processors can outperform their classical counterparts in certain applications. We review the latest progress and prospects in that effort, with the promise of advanced architectures and new technologies, such as microfabricated ion traps and integrated photonics.

Quantum physics can be distilled to two disjointed and counterintuitive rules. First, an isolated quantum system is represented by a "wave function," or a mathematical entity that evolves according to a wave equation and is shaped with external controls. Second, when a quantum system interacts with a measurement apparatus or its surrounding environment, the wave function probabilistically and irreversibly "collapses" into a particular state. The incompatibility of these two quantum rules is seen most clearly in a quantum superposition state, in which, for instance, an isolated particle's wave function is delocalized between two or more positions. The second rule ensures that such states are never directly seen in the macroscopic world. However, when a system is left isolated without interacting with its environment, the (microscopic) superposition persists and can be exploited to store massive amounts of information in parallel.

A quantum information processor encodes information in an array of quantum bits or qubits, which can hold superpositions of classical bit values 0 and 1. When N qubits are prepared in their most general state, we have a quantum superposition of all 2^N N-bit binary numbers. Such a superposition is typically "entangled" in the sense that certain qubit values are correlated with others, even though they yield random outcomes when measured individually. A quantum computer manipulates this exponential amount of information by interfering pieces of this complex superposition through controlled interactions, or quantum logic gate operations. A final measurement of the system can then yield information pertaining to all 2^N states. For merely $N = 400$ qubits, we find that the encoded information of $2^{400} \sim 10^{120}$ values is more than the number of fundamental particles in the universe; such a computation could never be performed without the parallel processing enabled by quantum mechanics. In a sense, entanglement between qubits acts as an invisible wiring that can potentially be exploited to solve certain problems that are intractable otherwise (*1*).

The requirements for large-scale quantum computer hardware are daunting, given the exponential sensitivity of such large superpositions to errors and leaks to the environment. However, there exist error-correction codes that allow arbitrarily complex quantum superposition states to be generated and stabilized (*1*), giving us hope that useful fault-tolerant quantum computers will eventually be realized despite the steep technical requirements far beyond current experimental capability.

In the search for quantum information processing hardware, one needs qubits that are extremely well isolated from the environment yet can be precisely controlled with external fields to affect interferences through the operations of quantum logic gates. Moreover, we must ultimately couple the qubits to the outside world in the strongest possible sense by performing a measurement that collapses any superposition onto definite values. These conflicting stringent requirements restrict potential quantum hardware to exotic microscopic systems. In this Review, we consider the most fundamental of these platforms—electromagnetically trapped atoms (*2*)—and speculate how this system may be scaled to hundreds or thousands of interacting qubits in the coming years.

Entangling Trapped Atomic Ion Qubits

Individual atoms are natural carriers of quantum information because they are standards: An isolated atom of carbon, for example, is exactly the same in Washington as it is in London or anywhere else. Isolation can be provided by confining atoms in an evacuated environment with electromagnetic traps, suspending atoms in free space so that they do not uncontrollably interact with background atoms, molecules, or surfaces. There are several compelling proposals for quantum computer architectures based on trapped neutral atoms and optical lattices, although the weak interaction between neutral atoms leads to difficulties in controlling their entanglement, and research in this area is still exploratory (*3*). Here, we focus on the trapping of electrically charged atoms, or ions, for which high-fidelity quantum operations and measurements are now commonplace.

The typical ion trap geometry for quantum information purposes is the linear radio frequency (rf) Paul trap, in which nearby electrodes hold static and dynamic electrical potentials that lead to an effective harmonic confinement of the ions, like a bowl full of mutually repelling marbles (*2*). When ions are laser-cooled to very low temperatures in such a trap, the ions form a linear crystal of qubits, with the Coulomb repulsion balancing the external confinement force (Fig. 1A). Ions are typically loaded into traps by creating a neutral atomic flux of the desired particle and ionizing them once in the trapping volume. Ions can remain confined for months, with lifetimes often limited by the level of vacuum. Elastic collisions with residual background gas occur roughly once per hour per ion at typical ultrahigh-vacuum pressures ($\sim 10^{-11}$ torr) and do not necessarily eject the ion, although inelastic collisions can change the species of the trapped ion. Cryogenic chambers can virtually eliminate these collision events by further reducing the background pressure.

Appropriate atomic ion species should have a strong closed optical transition that allows for laser-cooling of the motion, qubit state initialization, and efficient qubit readout. This rules out almost anything other than simple atomic ions with a lone outer electron, such as the alkaline-earths (Be^+, Mg^+, Ca^+, Sr^+, and Ba^+) and particular transition metals (Zn^+, Hg^+, Cd^+, and Yb^+). Qubits are represented by two stable electronic levels within each ion, sometimes characterized by an effective spin with the two states $|\uparrow\rangle$ and $|\downarrow\rangle$ corresponding to bit values 0 and 1.

The reduced energy level diagram of $^{171}Yb^+$ is shown in Fig. 2, B and C, in which the qubit levels $|\uparrow\rangle$ and $|\downarrow\rangle$ are represented by the stable hyperfine levels in the ground electronic state, separated by frequency $\nu_{HF} = 12.642\,812$ GHz. The excited electronic states $|e\rangle$ and $|e'\rangle$ are themselves split by a smaller hyperfine coupling and separated from the ground states by an optical interval. Laser radiation tuned just below resonance in these optical transitions allows Doppler laser cooling to confine ions near the bottom of the trap. Other more sophisticated forms of laser cooling can bring the ions to nearly at rest in the trap (*4*). When a bichromatic laser beam resonant with both $|\uparrow\rangle \leftrightarrow |e\rangle$ and $|\uparrow\rangle \leftrightarrow |e'\rangle$ transitions is applied to the atom, it rapidly falls into the state $|\downarrow\rangle$ and no longer interacts with the light

[1]Joint Quantum Institute (JQI), Department of Physics, University of Maryland, and National Institute of Standards and Technology, College Park, MD 20742, USA. [2]Department of Electrical and Computer Engineering, Duke University, Durham, NC 27708, USA. [3]Applied Quantum Technologies, Durham, NC 27707, USA.

*To whom correspondence should be addressed. E-mail: monroe@umd.edu

field (Fig. 1B), allowing the initialization of a qubit with essentially 100% fidelity. When a single laser resonant with the transition $|\uparrow\rangle \leftrightarrow |e\rangle$ is applied, the closed-cycling optical transition causes an ion in the $|\uparrow\rangle$ state to fluoresce strongly, whereas an ion in the $|\downarrow\rangle$ state stays dark because the laser is far from its resonance (Fig. 1C). The collection of even a small fraction of this fluoresence allows for the detection of the atomic qubit state with near-perfect efficiency. Other atomic species have similar initialization/detection schemes.

Coulomb-Based Gates and the Quantum CCD

The motion of many trapped ions is coupled through the Coulomb interaction, much like an array of pendulums connected by springs. A natural way to implement entangling quantum logic gates between ions in a crystal is thus to use the motion as an intermediary (Fig. 2A) by applying qubit state–dependent optical or microwave dipole forces to the ion (or ions) (*4*–*7*).

We assume that the qubit levels respond to an external field E by experiencing an equal and opposite energy shift $\pm\mu E$—for example, through the Stark effect for electric fields or the Zeeman effect for magnetic fields, in which case μ is an effective dipole moment of the qubit. When the field is inhomogeneous, this gives rise to a qubit state–dependent force along the x direction $F_x = \pm\mu E'(x)$, where the sign depends on the qubit state, and $E'(x)$ is the gradient of the applied field along x. For a plane wave radiation field with amplitude E_0 and wave vector k along x, $F_x = \pm hk\Omega$, where h is Planck's constant, and the Rabi frequency $\Omega = \mu E_0/h$ parametrizes the field-qubit coupling. Because this force acts differently on the two qubit states, it can coherently map the qubit state to the collective motion of N ions, with characteristic speed $R_{\mathrm{gate}} = \Omega\sqrt{\nu_R/\nu}$ (*4*, *7*). In this expression, $\nu_R = hk^2/(8\pi^2 M)$ is the recoil frequency of the ion crystal associated with momentum transfer from the field, M is the total mass of the ions, and ν is the frequency of harmonic oscillation of the collective motional mode along the x direction. Thus, a qubit superposition within the ion is transformed to a superposition of the ion's position. When applied to multiple ions, this fundamental operation allows gates to be performed between separated ions, mediated through the motion (*5*, *6*). Current experiments with a few ions have realized entangled state fidelities of greater than 99% (*8*) and operate in the range $R_{\mathrm{gate}} \sim 10$ to 100 kHz; with available ultrafast optical fields, it should be possible to operate gates in the gigahertz range (*9*).

As the number of ions N in the crystal grows, the gate speed slows down as $R_{\mathrm{gate}} \sim 1/\sqrt{N}$ from the mass term. For large crystals, there will also be crosstalk between the many modes of collective motion. Background errors such as the decoherence (heating) of the motional modes (*10*) or fluctuating fields that add random phases to the qubits will become important at longer times; thus, there will be practical limits on the size of a single crystal for the performance of faithful quantum gates. Individual optical addressing of ions (*11*) and pulse-shaping techniques (*12*) can mitigate these errors to achieve the full control of single crystals ranging from $N = 10$ to 100 qubits. This should allow the implementation of quantum simulations (*13*) in a regime in which classical modeling of certain many-body systems, such as frustrated spin networks, becomes intractable. It would also enable the construction of error-correcting encoded qubits that might form block primitives of an eventual fault-tolerant quantum computer.

In order to scale beyond 10 to 100 trapped ion qubits, we turn to a multiplexed architecture called the quantum charge-coupled device (QCCD) (*14*). This involves the sequential entanglement of small numbers of ions through their collective motion in a single chain and the classical shuttling of individual ions between different trapping zones to propagate the entanglement, as depicted in Fig. 2B. The QCCD architecture requires exquisite control of the ion positions during shuttling and may require additional atomic ion species to act as "refrigerator" ions to quench the excess motion from shuttling operations (*15*). Rudimentary versions of the QCCD idea have been used in many quantum information applications, such as teleportation and small quantum algorithms (*7*), and recent experiments have shown the reliable, repeatable, and coherent shuttling of ion qubits over millimeter distances in microseconds (*16*, *17*) and through complex two-dimensional junctions (Fig. 2, C and D) (*18*, *19*). The QCCD approach will push current state-of-the-art quantum information processing experiments to territories where elementary quantum error correction and simple quantum algorithms can be implemented. However, scaling to thousands or more qubits in the QCCD may be challenging because of the complexity of interconnects, diffraction of optical beams, and the extensive hardware required for qubit control.

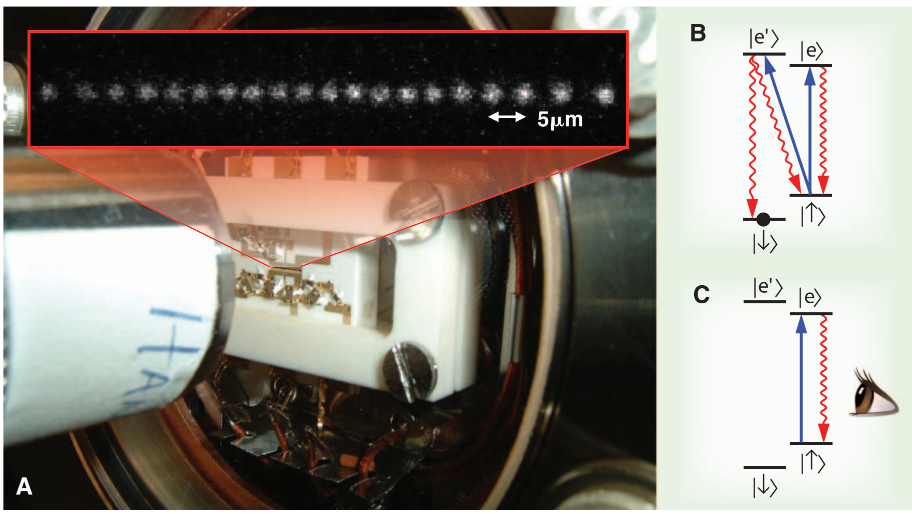

Fig. 1. (**A**) Vacuum chamber that houses electrodes for the trapping of atomic ions with a linear crystal of 20 confined atomic $^{171}Yb^{+}$ ions laser cooled to be nearly at rest. The atoms are illuminated with laser radiation tuned to a resonance in $^{171}Yb^{+}$, and the fluorescence is imaged onto a camera. The separation of the ions is determined by a balance between the external confinement force and Coulomb repulsion. (**B** and **C**) Reduced energy level diagram of each $^{171}Yb^{+}$ atomic ion, showing the atomic hyperfine levels $|\uparrow\rangle$ and $|\downarrow\rangle$ that represent a qubit. The electronic excited states $|e\rangle$ and $|e'\rangle$ are separated from the ground states by an energy corresponding to an optical wavelength of 369.53 nm, with all allowed transitions indicated by the downward red arrows. Applied laser radiation (upward blue arrows) drives these transitions for (B) initialization to state $|\downarrow\rangle$ and (C) fluorescence detection of the qubit state ($|\uparrow\rangle$, fluorescence, $|\downarrow\rangle$, no fluorescence).

Photonic Gates and Joining Remote Crystals

To scale beyond the QCCD in a modular architecture, one can link separate registers of trapped ion chains with photonic interfaces. In this scheme, an entangled qubit pair is first generated between the two registers, which is then used to implement a two-qubit gate between two ions that belong to each register (*20*). This approach is not limited to trapped ions and can be generalized to other physical systems with strong optical transitions (*3*).

A pair of trapped ion qubit registers [termed elementary logic units (ELUs)] can be entangled with each other by using propagating photons emitted by a subset of ions from each register, designated to be "communication qubits." Each communication qubit is driven to an excited state with near unit probability $p_e \sim 1$ by using a fast laser pulse, so that at most one photon emerges following appropriate radiative selection rules (Fig. 2E). The photon carries its qubit through two distinguishable internal photonic states (such as polarization or optical frequency) (*21*, *22*). For example, the joint state of a communication qubit and emitted photonic qubit can be written $|\downarrow\rangle_i|\nu_\downarrow\rangle_i + |\uparrow\rangle_i|\nu_\uparrow\rangle_i$, where $|\nu_\downarrow\rangle_i$ and $|\nu_\uparrow\rangle_i$ denote the frequency qubit states of a single photon

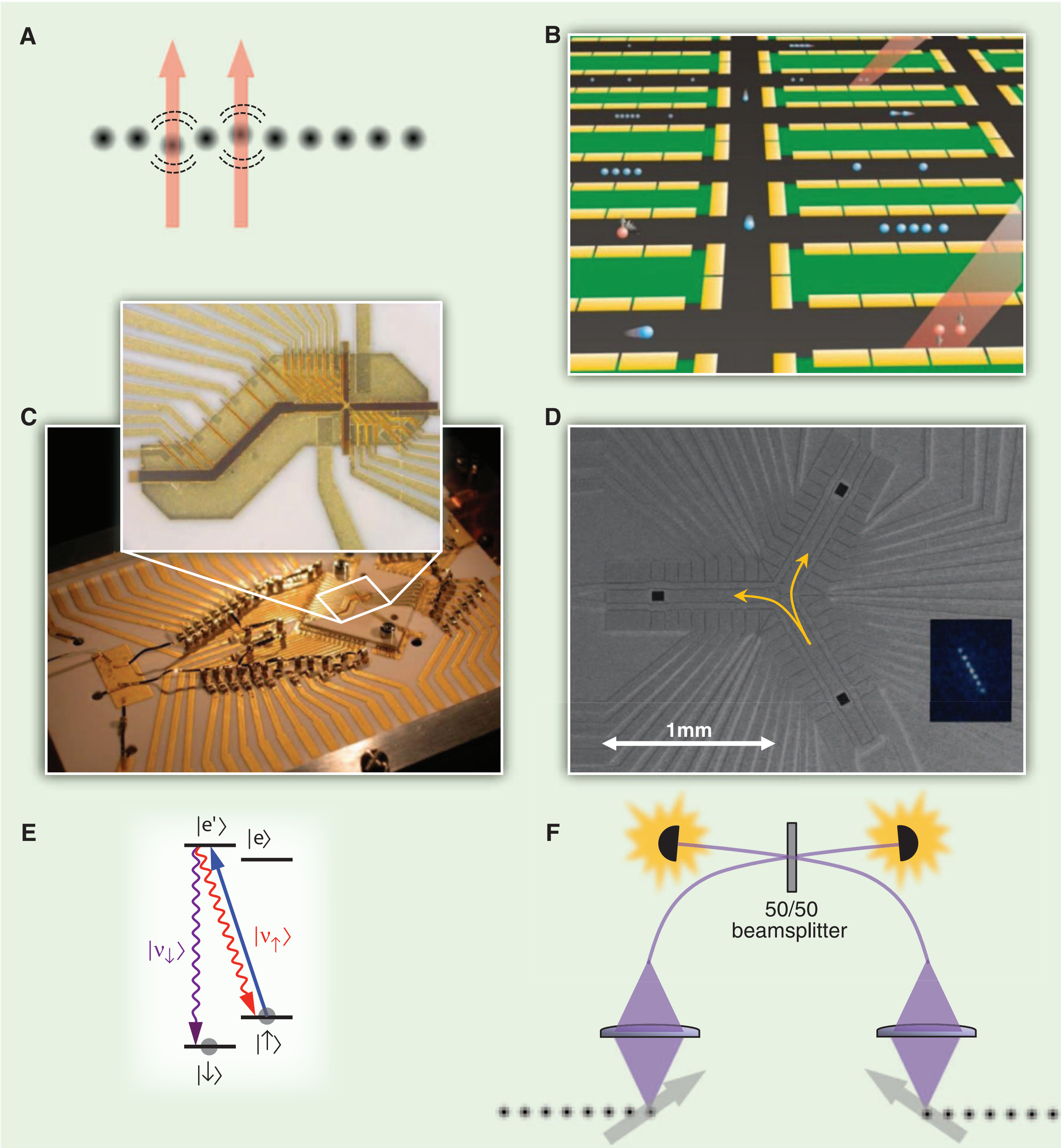

Fig. 2. (**A**) Optical dipole forces (red) displace two ions depending on their qubit states, and the resulting modulation of the Coulomb interaction allows the implementation of the controlled-NOT gate between these two ions. (**B**) Concept of a quantum CCD trap, in which ions can be shuttled between various zones. Ions can be entangled within a small crystal using laser forces as in (A) and then moved to different zones to propagate the entanglement to other ion crystals. Additional zones can be used for the loading of ions or qubit state detection. In principle, any pair of ions can be brought together through a web of ion trap channels, and a separate ion species can be used for sympathetic cooling to quench any residual motion from the shuttling procedure. [Image credit: National Institute of Standards and Technology] (**C**) Ion trap structure for the shuttling of ions through a junction. [Main image adapted with permission from (*18*); copyright 2011 by the American Physical Society] (**D**) Surface ion trap structure for shuttling ions through a three-channel junction. Inset shows an image of a trapped ion chain in lower right-hand sector. [Adapted with permission from (*19*); publisher: Institute of Physics] (**E**) Energy levels of trapped ion excited with a fast laser pulse (blue upward arrow) that produces single photon whose color, represented by the state $|\nu_\uparrow\rangle$ or $|\nu_\downarrow\rangle$, is entangled with the resultant qubit state $|\uparrow\rangle$ or $|\downarrow\rangle$, respectively. (**F**) Two "communication qubit" ions, immersed in separate crystals of other ions, each produce single photons when driven by laser pulses (blue). With some probability, the photons arrive at the 50/50 beamsplitter and then interfere. If the photons are indistinguishable (in polarization and color), then they always leave the beamsplitter along the same path. The simultaneous detection of photons at the two output detectors means that the photons were different colors, but because there is no knowledge of which color photon came from which ion emitter, this coincidence detection heralds the entanglement of the trapped ion qubits.

emitted by the i-th communication qubit. Here, we assume that the two photonic frequencies are distinguishable, or $|\nu_\uparrow - \nu_\downarrow| >> \gamma$, where γ is the radiative linewidth of the excited state. When two communication qubits i and j are excited in this way, and their photons are mode-matched on a 50/50 beamsplitter (Fig. 2F), the entanglement of the memories is heralded by the joint (coincidence) detection of photons at output detectors, creating the entangled state $|\downarrow\rangle_i|\uparrow\rangle_j - |\uparrow\rangle_j|\downarrow\rangle_i$ (*21–24*). This entanglement link succeeds with probability $p = (p_e F\eta_D)^2/2$, where F is the fraction of light collected from each emitter, and η_D is the single photon detector efficiency. Even though this is a probabilistic link, the detected photons indicate success, and the resulting entanglement between the ions can subsequently be used for deterministic quantum information processing. The mean connection rate is given by Rp, where R is the repetition rate of the initialization/excitation process, limited by the emission rate γ. For typical atomic transitions into free space with $\gamma \sim 10^8$/s, light collection fraction $F \sim 1$ to 10%, and detector efficiency $\eta_D \sim 20\%$, we find typical connection rates of 1 to 1000 Hz, with substantial gains possible with better photon collection strategies (*25*).

In practice, the communication qubit must be well isolated from the neighboring memory qubit ions so that scattered light from the excitation laser or the emitted photons themselves do not disturb the other memory qubits in each register. Although physical separation of the ions can provide the requisite isolation, a better solution is to use two different atomic species (*26*) to eliminate this crosstalk—for instance, $^{171}Yb^+$ for the memory qubit and $^{138}Ba^+$ for the communication qubit. Here, the communication qubits from separate registers become entangled via the photonic channel, and then the qubits within the communication ions are coherently mapped to neighboring memory qubits through Coulomb gates as described above.

New Technology for Scalability and Modularity

Scalable ion traps will require precision electrode structures, with as many discrete electrodes as trapped ion qubits, suggesting the use of micrometer-scale surface chip traps (*27*, *28*) that can be fabricated by using standard semiconductor processing techniques (*29*). Highly complex surface traps that can handle several tens of ions over tens of trapping zones have been fabricated and tested (Fig. 3, A and B) (*19*, *30*, *31*), with loading of up to ~10 ions with high-fidelity qubit preparation, detection, and single-qubit gate operations. Multi-qubit entangling operations in microscopic traps are more challenging because the ions experience higher levels of electric field noise from closer electrodes, causing motional decoherence during the gate operation. Although the source of this noise is still not well understood (*10*), it seems to scale roughly as $1/d^4$, where d is the characteristic distance from the ions to the nearest electrode (*32*). This motional heating can be quenched at cryogenic temperatures (*32*, *33*) or with adequate treatment of the trap surface (*34*), so this problem does not appear to be a fundamental limitation.

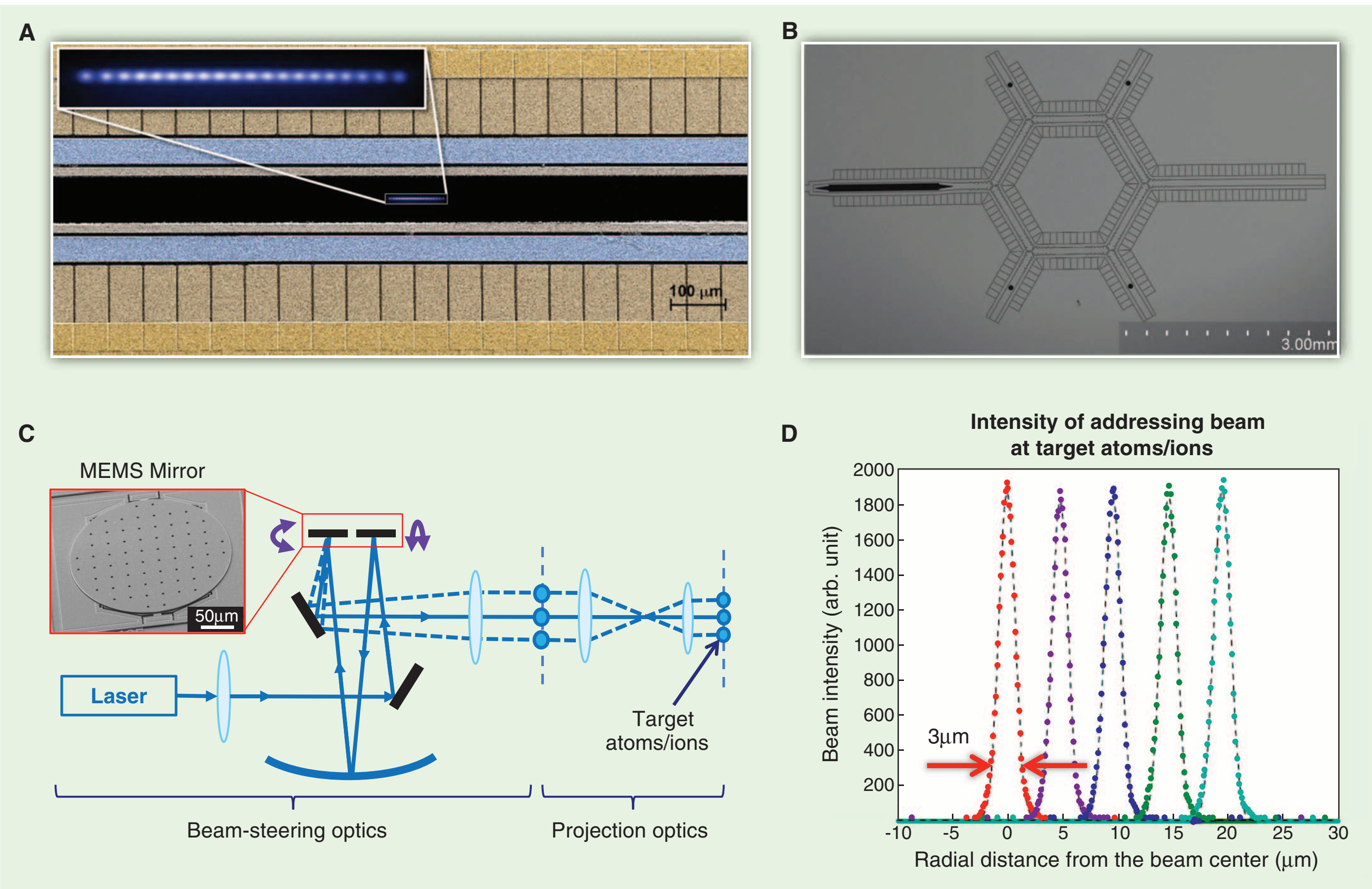

Fig. 3. (**A**) Scanning electron micrograph of a microfabricated linear trap with a long slot, with superimposed image of 20-ion chain in an anharmonic well (inset). The blue rails are RF electrodes and the rest are segments of static electrodes. [Courtesy GTRI] (**B**) Circulator trap with six junctions and two linear sections on either side for qubit manipulation. The other four short sections can be used as loading zones (of multiple ion species, if necessary), and the six junctions enable reordering of ions in the chain. [Courtesy Sandia National Laboratories] (**C**) Technology for individual optical addressing of ions in a linear chain. A control laser beam bounces off two MEMS mirrors tilting in orthogonal directions (inset) and can be steered over a two-dimensional space at the target atoms or ions. (**D**) The resulting profile of a ~3-µm diameter beam at 369.5 nm with a steering range of ~20 µm measured at the site of the ions.

Although the technology of trapping large numbers of ions has progressed, scaling the ability to individually address the qubits in the chain remains a challenge. Individual addressing of single atoms in an array via steering the control beam by using either electro-optic (EO) or acousto-optic deflectors has been demonstrated for small arrays (*35*, *36*). For larger atomic arrays, fast scanning mirrors provide an attractive solution (*37*, *38*). The advances in micro-electromechanical systems (MEMS) technology enable micromirror-based optical systems capable of independently steering multiple beams over the same atomic array (Fig. 3C).

A single ion chain (or several chains on a chip connected through the QCCD architecture) with an optical interface (Fig. 2F) can serve as a processor node (ELU) of a distributed quantum multicomputer, in which two-qubit gates between ions that belong to different ELUs are realized by using the photonic gate (*39*). When a large number ($\sim10^3$) of such ELUs are connected through a reconfigurable photonic network supported by an optical crossconnect switch (*40*), a scalable quantum computer with up to $\sim10^6$ qubits can be constructed (Fig. 4A). This architecture allows entanglement between any pair of ELUs in the processor with operations running in parallel, and distance-independent logic gate operations between any two qubits in the system. Such features are crucial for efficiently executing quantum algorithms that require nonlocal gates among the qubits and ensuring fault-tolerant quantum computation (*39*).

By conveying the photonic link over long distances, entanglement can be distributed between high-quality ion memory qubits separated by the distance traveled by the photons. Combined with the ability to perform local logic gates and high-fidelity measurements, each chip can thus serve as a quantum repeater node (Fig. 4B) that enables distribution of quantum entanglement over macroscopic distances by means of successive entanglement swapping (*41*). The photons adequate for carrying quantum information from ion qubits tend to have wavelengths in the ultraviolet or in the visible part of the spectrum, which is far from ideal for long-distance transmission. Quantum frequency converters can be used to translate the wavelength of the photon for better transmission (*42*). Shown in Fig. 4C is a schematic of a chain of quantum repeaters that enable entangled qubit pair distribution over macroscopic distances, which can be used for various quantum communication protocols, including quantum key distribution (QKD).

A major challenge in both modular quantum computer and quantum repeater applications is the slow rate of entanglement generation for the photonic gate, which is dominated by the low collection efficiency of the emitted photons. Continual efforts to improve collection of emitted photons into a single-mode fiber, involving the integration of ion traps with optical components such as mirrors (*43*), high numerical aperture lenses (*44*), and optical cavities (*45*), may boost the entanglement generation rate up by several orders of magnitude to above the decoherence rates of ion qubits.

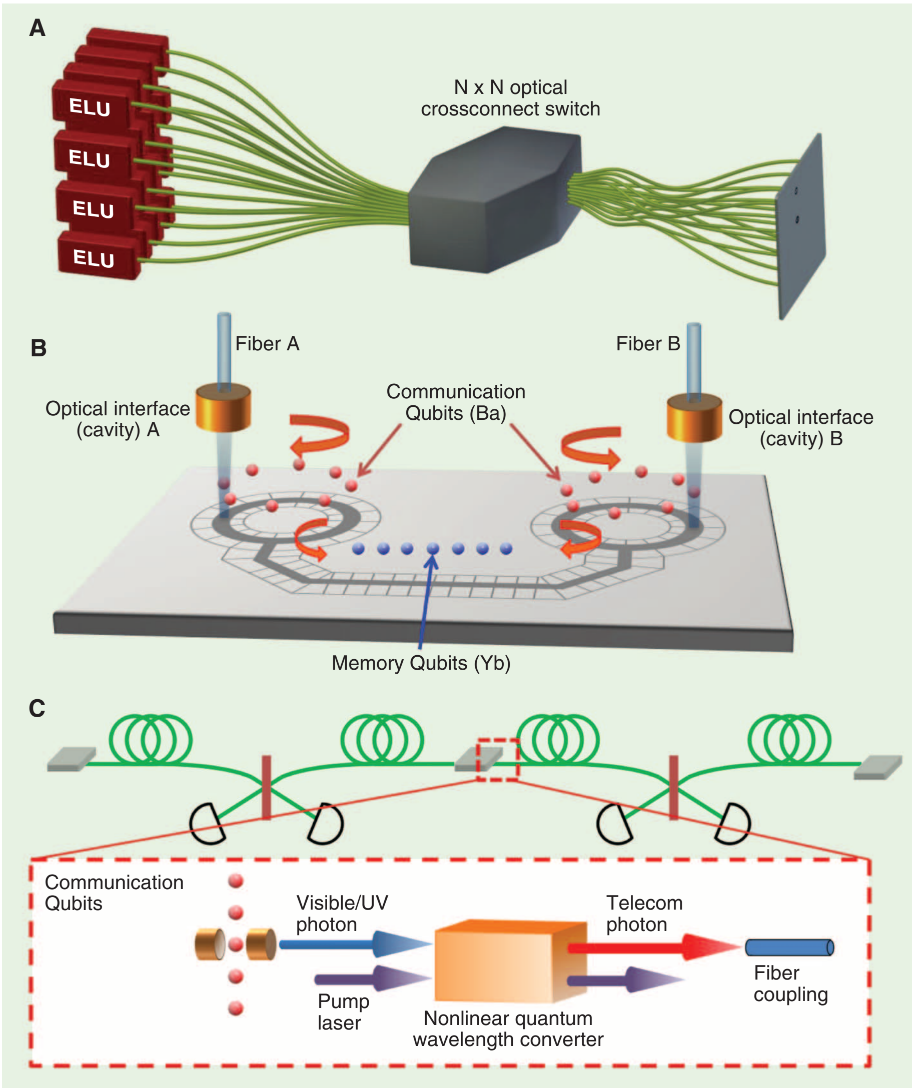

Fig. 4. Advanced quantum information systems with trapped ion technology. **(A)** Modular distributed quantum computer. Several ELUs are connected through a photonic network by using an optical crossconnect switch, inline fiber beamsplitters, and a photon-counting imager (*39*). [Adapted with permission from (*46*)] **(B)** Trapped ion quantum repeater node made up of communication qubit ions (such as Ba^+) and memory qubit ions (such as Yb^+), with two optical interfaces per node. Multiple communication qubits are used per optical interface to inject photons into the optical channel, while the results for successful entanglement generation at the detectors are reported back to this node. Only qubits corresponding to successful events will be transported to the memory qubit region for use in quantum repeater protocol. **(C)** A chain of quantum repeater nodes can distribute quantum entanglement over macroscopic distances. The photons generated by the ions must be converted to telecommunication wavelengths for long-distance transport, which can be achieved by nonlinear optical processes.

Outlook

The past decade has seen a number of small quantum information processors based on trapped ions, but in the coming years, we may see trapped ion devices used for applications that are difficult or impossible to perform using conventional technology. A quantum simulator that involves more than ~30 qubits may soon be able to predict behavior of interacting spin systems that is not tractable by a classical computer. Distribution of high-quality entangled qubit pairs over macroscopic distances by using trapped ion quantum repeaters may lead to new applications, such as long-distance QKD and multipartite entanglement distribution, as well as fundamental results, such as a loophole-free test of quantum nonlocality.

With the advent of microfabricated ion trap chips integrated with photonic components, modular ion trap quantum computer architectures may lead to even larger quantum computers that can ultimately be put to use in materials design, communications, and high-performance computation. As quantum systems are made ever larger, they ultimately tend toward classical behavior because the quantum nature of the system quickly disappears even at the presence of tiny amounts of dissipation. Whether we find that the strange rules of quantum physics indeed persist to much larger systems, or perhaps a new order emerges, the trapped ion platform for quantum information processing is expected to provide the leading experimental playground in which to explore the evolution of complex quantum systems.

References and Notes

1. M. A. Nielsen, I. L. Chuang, *Quantum Computation and Quantum Information* (Cambridge Univ. Press, Cambridge, 2000).
2. C. R. Monroe, D. J. Wineland, *Sci. Am.* **299**, 64 (2008).
3. T. D. Ladd *et al.*, *Nature* **464**, 45 (2010).
4. D. Leibfried, R. Blatt, C. Monroe, D. Wineland, *Rev. Mod. Phys.* **75**, 281 (2003).
5. J. I. Cirac, P. Zoller, *Phys. Rev. Lett.* **74**, 4091 (1995).
6. A. Sørensen, K. Mølmer, *Phys. Rev. Lett.* **82**, 1971 (1999).
7. R. Blatt, D. Wineland, *Nature* **453**, 1008 (2008).
8. J. Benhelm, G. Kirchmair, C. F. Roos, R. Blatt, *Nat. Phys.* **4**, 463 (2008).
9. J. J. García-Ripoll, P. Zoller, J. I. Cirac, *Phys. Rev. Lett.* **91**, 157901 (2003).
10. Q. A. Turchette *et al.*, *Phys. Rev. A* **61**, 063418 (2000).
11. H. Häffner, C. Roos, R. Blatt, *Phys. Rep.* **469**, 155 (2008).
12. S.-L. Zhu, C. Monroe, L.-M. Duan, *Europhys. Lett.* **73**, 485 (2006).
13. J. Ignacio Cirac, P. Zoller, *Nat. Phys.* **8**, 264 (2012).
14. D. Kielpinski, C. Monroe, D. J. Wineland, *Nature* **417**, 709 (2002).
15. M. D. Barrett *et al.*, *Phys. Rev. A* **68**, 042302 (2003).
16. A. Walther *et al.*, *Phys. Rev. Lett.* **109**, 080501 (2012).
17. R. Bowler *et al.*, *Phys. Rev. Lett.* **109**, 080502 (2012).
18. R. B. Blakestad *et al.*, *Phys. Rev. A* **84**, 032314 (2011).
19. D. L. Moehring *et al.*, *New J. Phys.* **13**, 075018 (2011).
20. D. Gottesman, I. L. Chuang, *Nature* **402**, 390 (1999).
21. C. Simon, W. T. M. Irvine, *Phys. Rev. Lett.* **91**, 110405 (2003).
22. D. L. Moehring *et al.*, *Nature* **449**, 68 (2007).
23. C. Cabrillo, J. I. Cirac, P. Garcia-Fernandez, P. Zoller, *Phys. Rev. A* **59**, 1025 (1999).
24. L. Slodicka *et al.*, http://arxiv.org/abs/1207.5468 (2012).
25. T. Kim, P. Maunz, J. Kim, *Phys. Rev. A* **84**, 063423 (2011).
26. P. O. Schmidt *et al.*, *Science* **309**, 749 (2005).
27. J. Chiaverini *et al.*, *Quant. Inf. Comp.* **5**, 419 (2005).
28. S. Seidelin *et al.*, *Phys. Rev. Lett.* **96**, 253003 (2006).
29. J. Kim *et al.*, *Quant. Inf. Comput.* **5**, 515 (2005).
30. J. Amini *et al.*, *New J. Phys.* **12**, 033031 (2010).
31. J. T. Merrill *et al.*, *New J. Phys.* **13**, 103005 (2011).
32. L. Deslauriers *et al.*, *Phys. Rev. Lett.* **97**, 103007 (2006).
33. J. Labaziewicz *et al.*, *Phys. Rev. Lett.* **101**, 180602 (2008).
34. D. A. Hite *et al.*, *Phys. Rev. Lett.* **109**, 103001 (2012).
35. F. Schmidt-Kaler *et al.*, *Nature* **422**, 408 (2003).
36. D. D. Yavuz *et al.*, *Phys. Rev. Lett.* **96**, 063001 (2006).
37. C. Knoernschild *et al.*, *Appl. Phys. Lett.* **97**, 134101 (2010).
38. C. Weitenberg *et al.*, *Nature* **471**, 319 (2011).
39. C. Monroe *et al.*, http://arxiv.org/abs/1208.0391 (2012).
40. J. Kim *et al.*, *IEEE Photon. Technol. Lett.* **15**, 1537 (2003).
41. H.-J. Briegel, W.Dür, J. I. Cirac, P. Zoller, *Phys. Rev. Lett.* **81**, 5932 (1998).
42. K. De Greve *et al.*, *Nature* **491**, 421 (2012).
43. P. F. Herskind *et al.*, *Opt. Lett.* **36**, 3045 (2011).
44. A. Jechow, E. W. Streed, B. G. Norton, M. J. Petrasiunas, D. Kielpinski, *Opt. Lett.* **36**, 1371 (2011).
45. M. Steiner, H. M. Meyer, C. Deutsch, J. Reichel, M. Köhl, http://arxiv.org/abs/1211.0050 (2012).
46. L.-M. Duan, C. Monroe, *Rev. Mod. Phys.* **82**, 1209 (2010).

Acknowledgments: This work was supported by the U.S. Army Research Office (ARO) award W911NF0710576 with funds from the Defense Advanced Research Projects Agency (DARPA) Optical Lattice Emulator Program, ARO award W911NF0410234 with funds from the Intelligence Advanced Research Projects Activity Multi-Qubit Coherent Operations program, ARO Multidisciplinary University Initiative award W911NF0910406 on Hybrid Quantum Optical Circuits, Army Contracting Command award W31P4Q1210017 with funds from the DARPA Quiness Program, and the NSF Physics Frontier Center at JQI.

10.1126/science.1231298

REVIEW

Superconducting Circuits for Quantum Information: An Outlook

M. H. Devoret[1,2] and R. J. Schoelkopf[1]*

The performance of superconducting qubits has improved by several orders of magnitude in the past decade. These circuits benefit from the robustness of superconductivity and the Josephson effect, and at present they have not encountered any hard physical limits. However, building an error-corrected information processor with many such qubits will require solving specific architecture problems that constitute a new field of research. For the first time, physicists will have to master quantum error correction to design and operate complex active systems that are dissipative in nature, yet remain coherent indefinitely. We offer a view on some directions for the field and speculate on its future.

The concept of solving problems with the use of quantum algorithms, introduced in the early 1990s (*1*, *2*), was welcomed as a revolutionary change in the theory of computational complexity, but the feat of actually building a quantum computer was then thought to be impossible. The invention of quantum error correction (QEC) (*3*–*6*) introduced hope that a quantum computer might one day be built, most likely by future generations of physicists and engineers. However, less than 20 years later, we have witnessed so many advances that successful quantum computations, and other applications of quantum information processing (QIP) such as quantum simulation (*7*, *8*) and long-distance quantum communication (*9*), appear reachable within our lifetime, even if many discoveries and technological innovations are still to be made.

Below, we discuss the specific physical implementation of general-purpose QIP with superconducting qubits (*10*). A comprehensive review of the history and current status of the field is beyond the scope of this article. Several detailed reviews on the principles and operations of these circuits already exist (*11*–*14*). Here, we raise only a few important aspects needed for the discussion before proceeding to some speculations on future directions.

Toward a Quantum Computer

Developing a quantum computer involves several overlapping and interconnecting stages (Fig. 1). First, a quantum system has to be controlled sufficiently to hold one bit of quantum information long enough for it to be written, manipulated, and read. In the second stage, small quantum algorithms can be performed; these two stages require that the first five DiVincenzo criteria be satisfied (*15*). The following, more complex stages, however, introduce and require QEC (*3*–*6*). In the third stage, some errors can be corrected by quantum nondemolition readout of error syndromes such as parity. It also becomes possible to stabilize the qubit by feedback into any arbitrary state (*16*, *17*), including dynamical ones (*18*–*21*). This stage was reached first by trapped ions (*22*), by Rydberg atoms (*16*), and most recently by superconducting qubits (*23*–*25*). In the next (fourth) stage, the goal is to realize a quantum memory, where QEC realizes a coherence time that is longer than any of the individual components. This goal is as yet unfulfilled in any system. The final two stages in reaching the ultimate goal of fault-tolerant quantum information processing (*26*) require the ability to do all single-qubit operations on one logical qubit (which is an effective qubit protected by active error correction mechanisms), and the ability to perform gate operations between several logical qubits; in both stages the enhanced coherence lifetime of the qubits should be preserved.

Superconducting Circuits: Hamiltonians by Design

Unlike microscopic entities—electrons, atoms, ions, and photons—on which other qubits are based, superconducting quantum circuits are based on the electrical (LC) oscillator (Fig. 2A) and are macroscopic systems with a large number

[1]Departments of Applied Physics and Physics, Yale University, New Haven, CT 06520, USA. [2]College de France, Place Marcelin Berthelot, F-75005 Paris, France.

*To whom correspondence should be addressed. E-mail: robert.schoelkopf@yale.edu